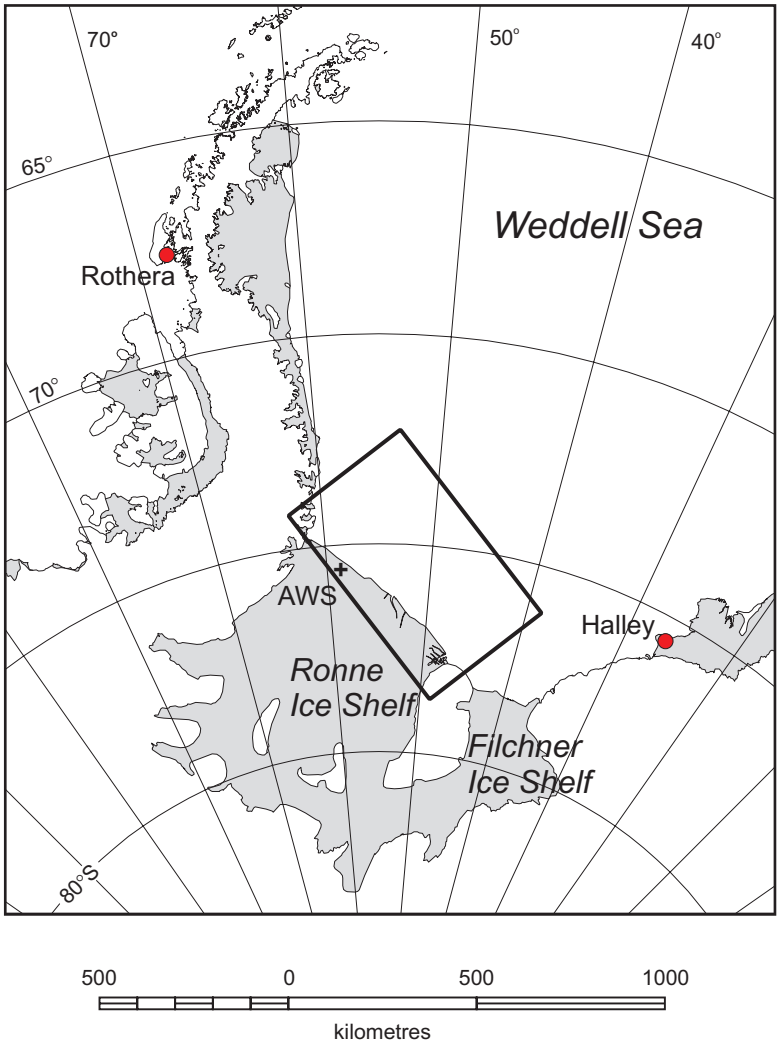


Figure 1 A map of the southern Weddell Sea region. The study region is marked by the inner rectangle.

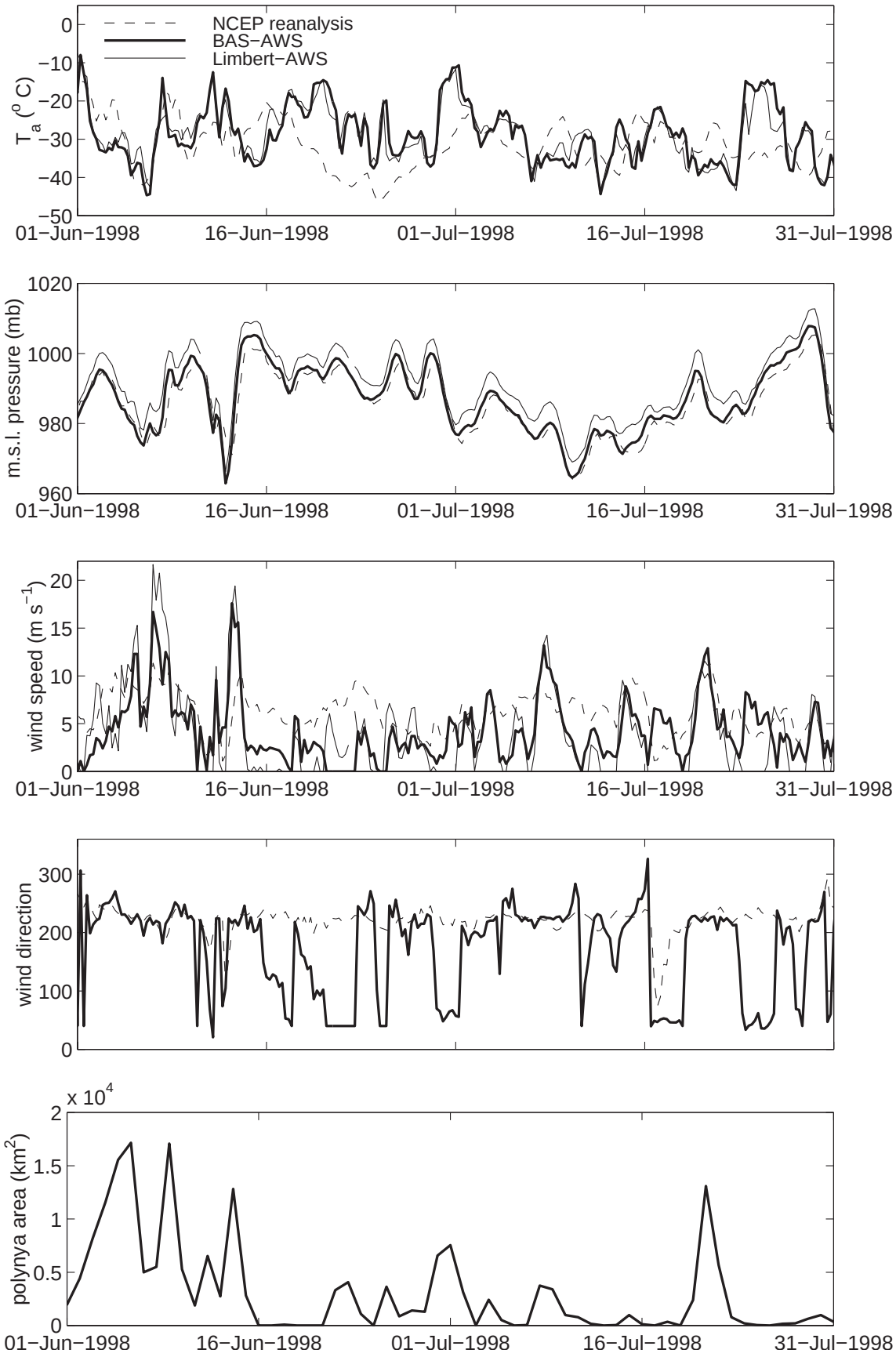


Figure 2 Time series of June-July 1998 showing data from the BAS-AWS, the Limbert-AWS and extracted from the NCEP/NCAR reananlysis. The panels plot: 2 m air temperature, m.s.l. pressure, 3 m wind speed, and wind direction. The final panel shows coastal polynya area from the PSSM data.

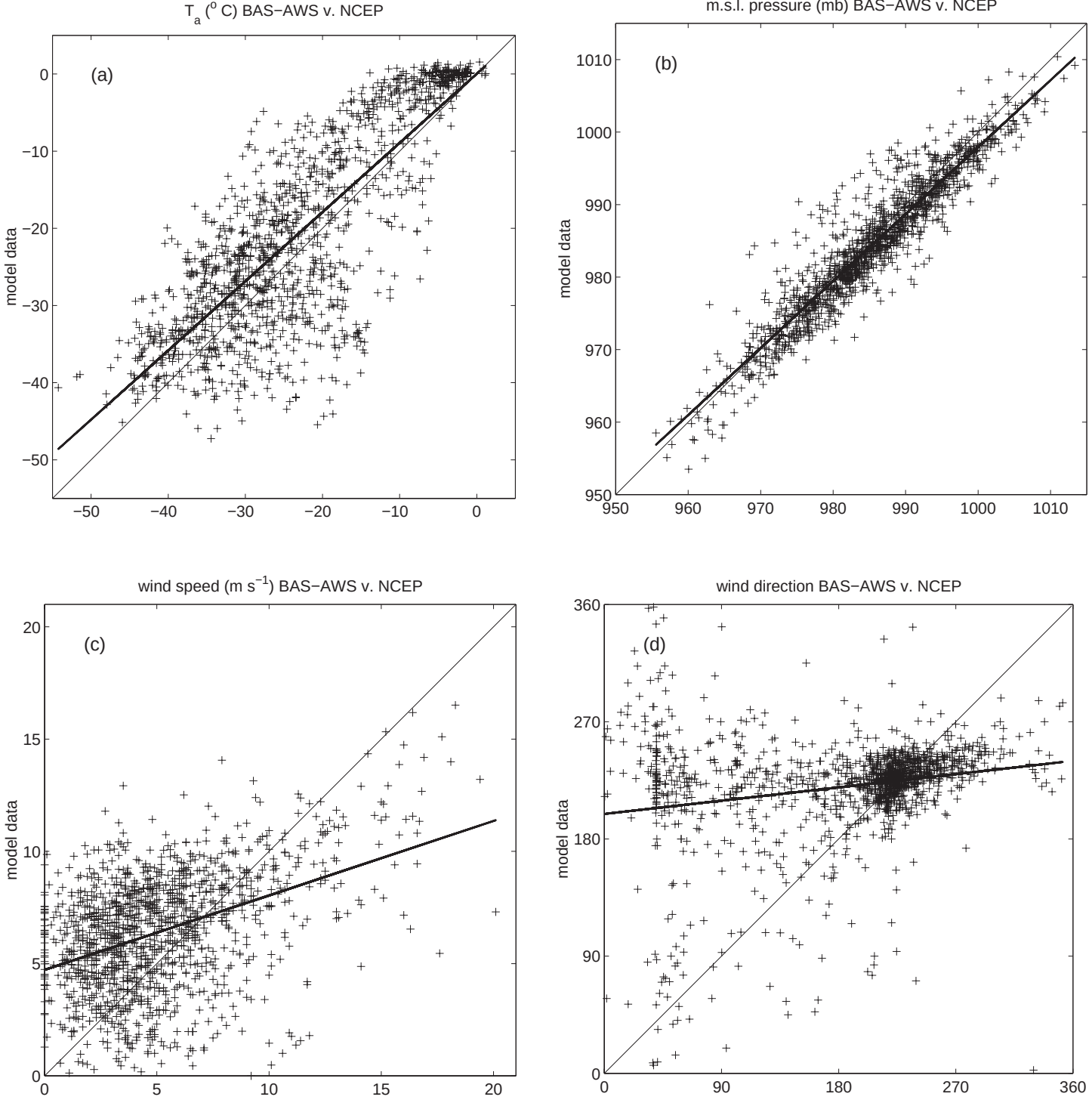


Figure 3 Scatter plots comparing data from the BAS-AWS and from the NCEP/NCAR reanalysis. The period of comparison is 1 February to 31 December 1998. A linear regression line is overlain. The panels are (a) 2-m air temperature, (b) m.s.l. pressure, (c) 3-m wind speed and (d) wind direction.

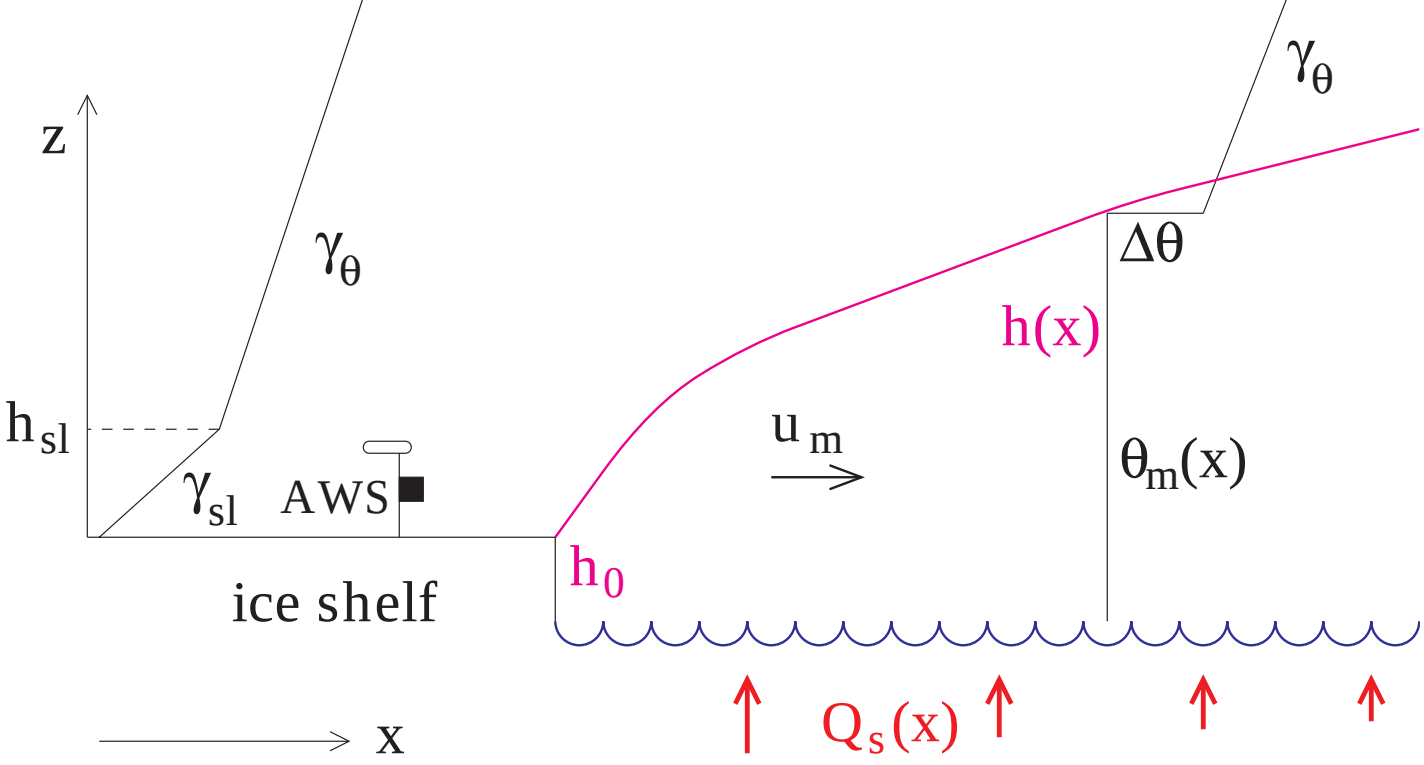


Figure 4 A sketch of a convective-thermal internal boundary layer development for a cold air outbreak over a polynya. The Renfrew and King (2000) model predicts CIBL height *h(x)*, mixed-layer potential temperature θ_m, and surface sensible heat flux $Q_s(x)$ from upstream surface data, given an inital CIBL height h_0, a surface-layer height h_{sl}, and stabilities γ_θ and γ_{sl}.

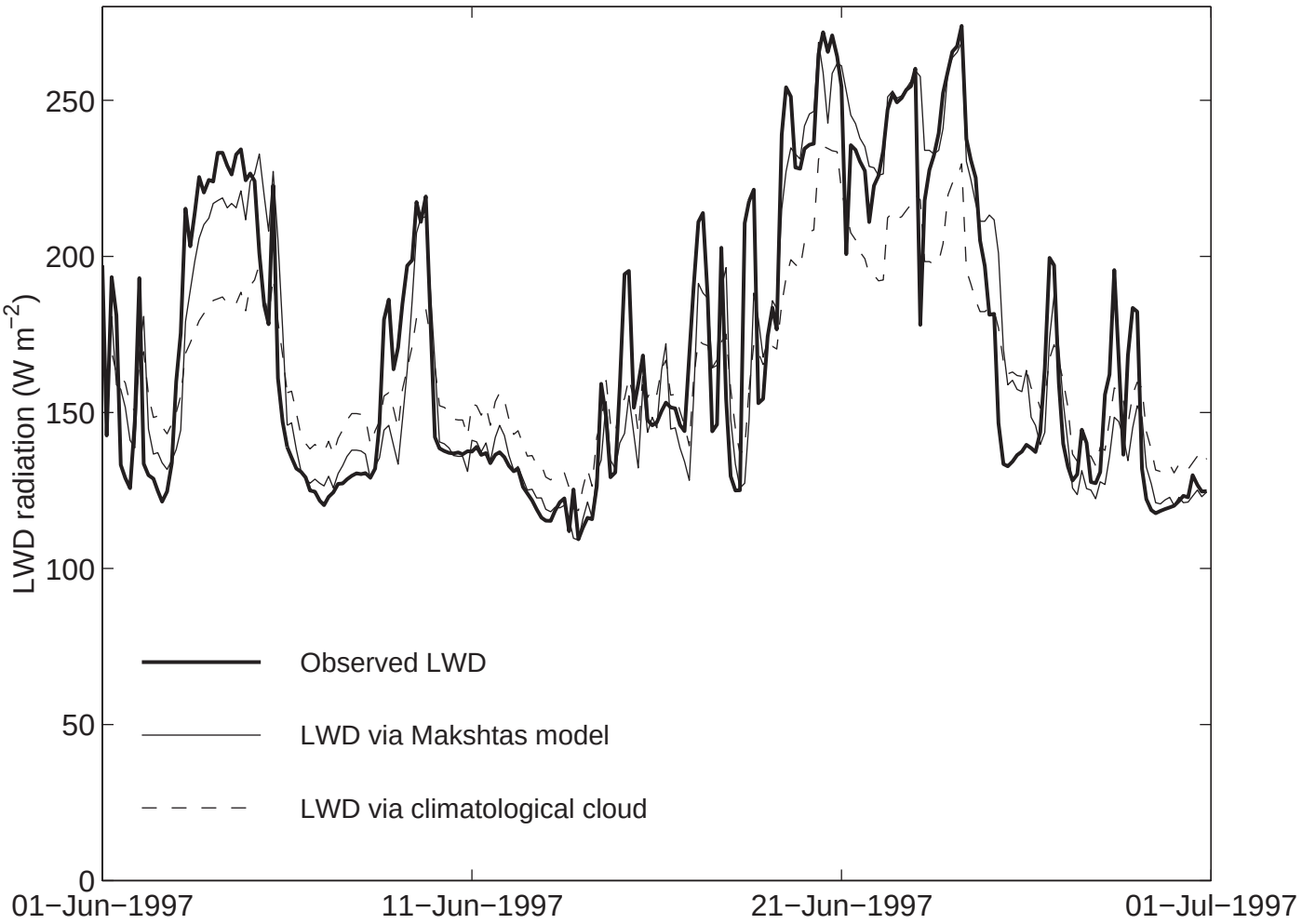


Figure 5 Time series from June 1997 of LWD radiation at Halley Base. The plot compares the observed LWD with those calculated via eqn. (4) firstly using the Makshtas et al. (1999) cloud model, and secondly using a climatological cloud cover.

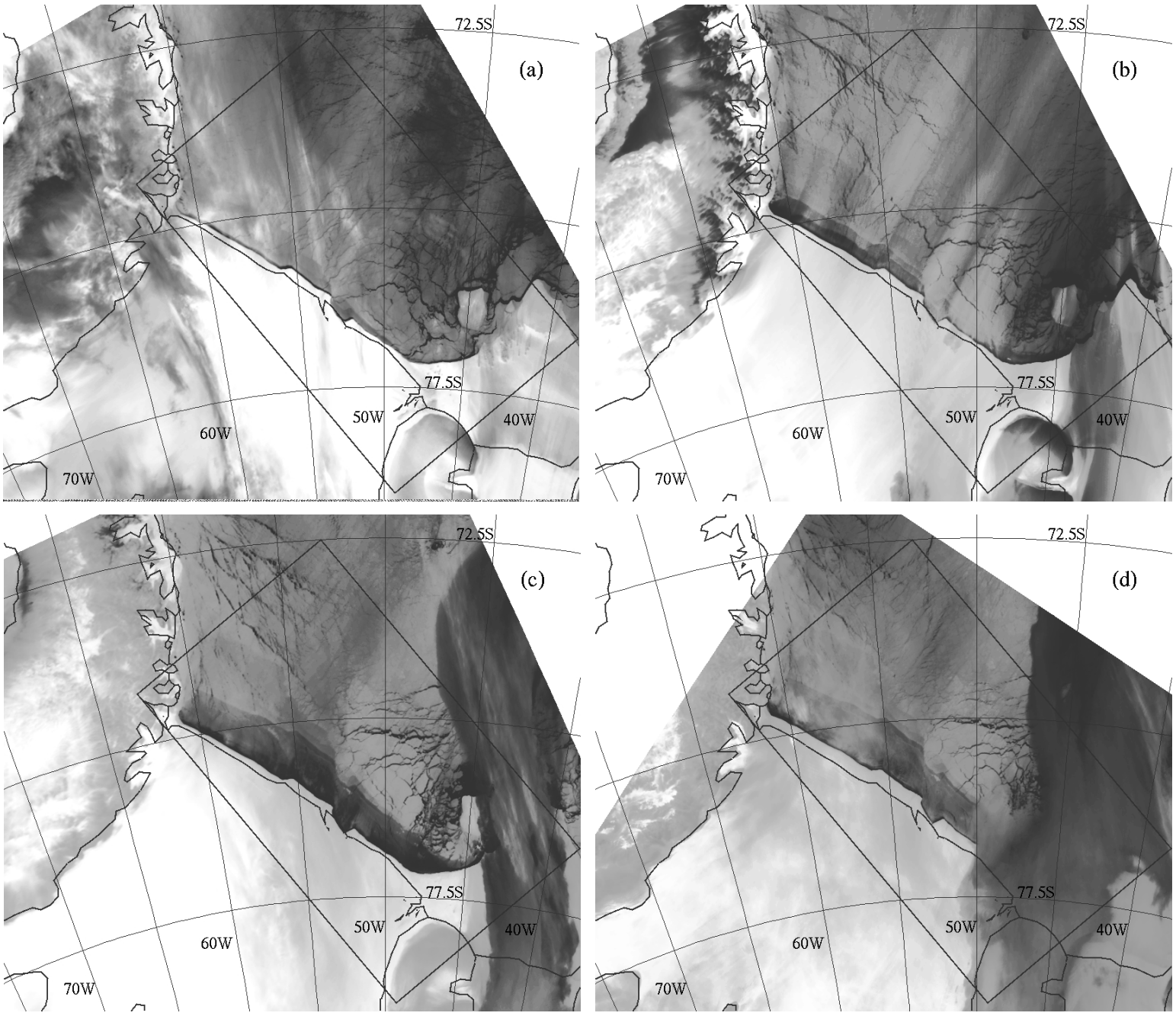


Figure 6 Infra-red AVHRR satellite images of the southern Weddell Sea and the Ronne Ice Shelf, processed so that white is cold, black is warm. The images show a coastal polynya opening episode, with sea ice being blown off the ice shelf, exposing a belt of warmer open water underneath. The panels are from (a) 19.53 UTC 19th July 1998, (b) 19.42 20th July, (c) 19.30 21st July and (d) 3.51 22nd July. The inner rectangle superimposed on the image shows the area processed via the PSSM algorithm. Note the dark band on the right of images (b)-(d) is a due to a relatively warm band of cloud.

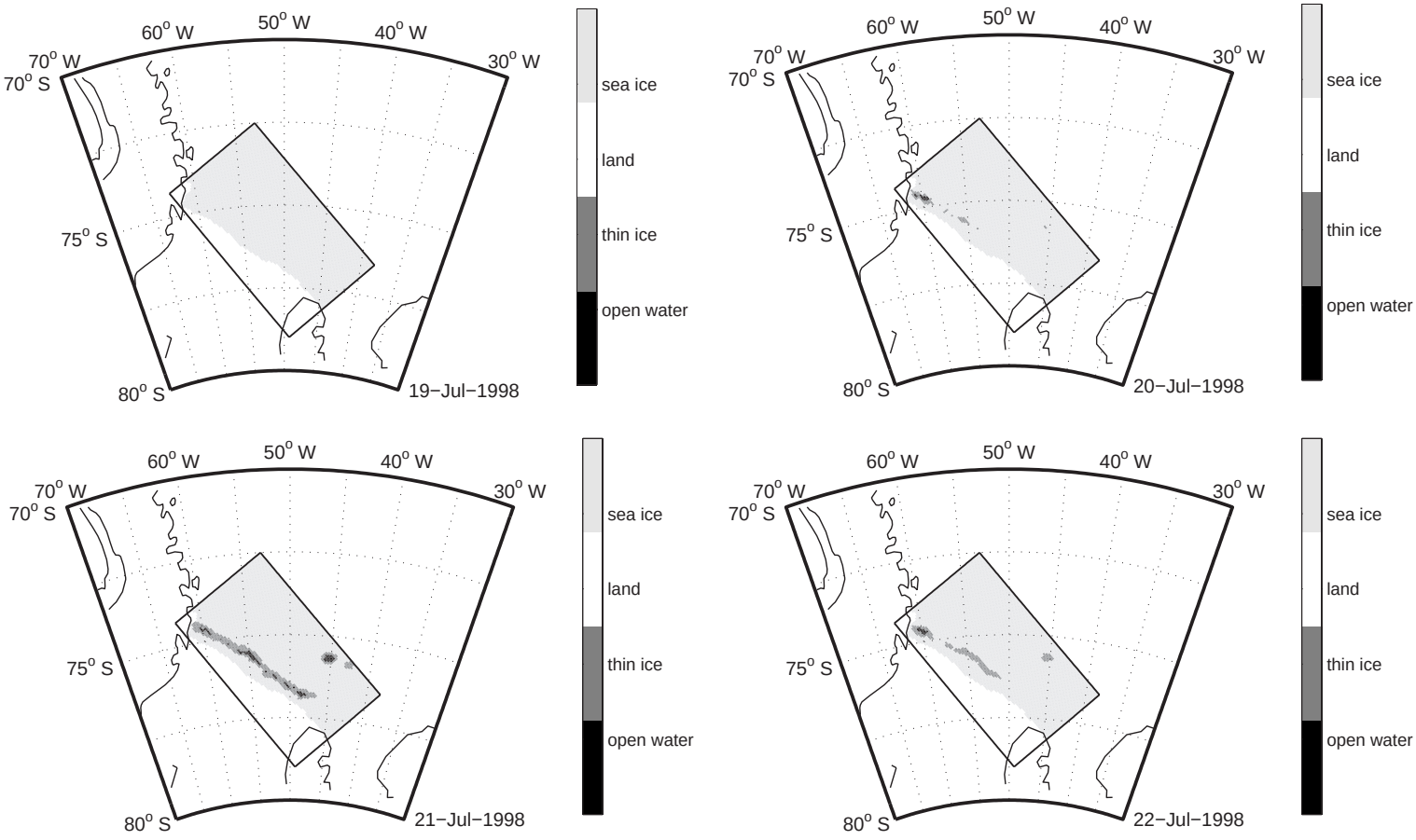


Figure 7 Maps of sea ice cover as determined by the PSSM algorithm from SSMI passive microwave brightness temperatures. The inner rectangle shows the region processed. The algorithm differentiates regions of open water and thin ice from those of thicker sea ice. The panels are for 19th, 20th, 21st and 22nd July 1998 as indicated.

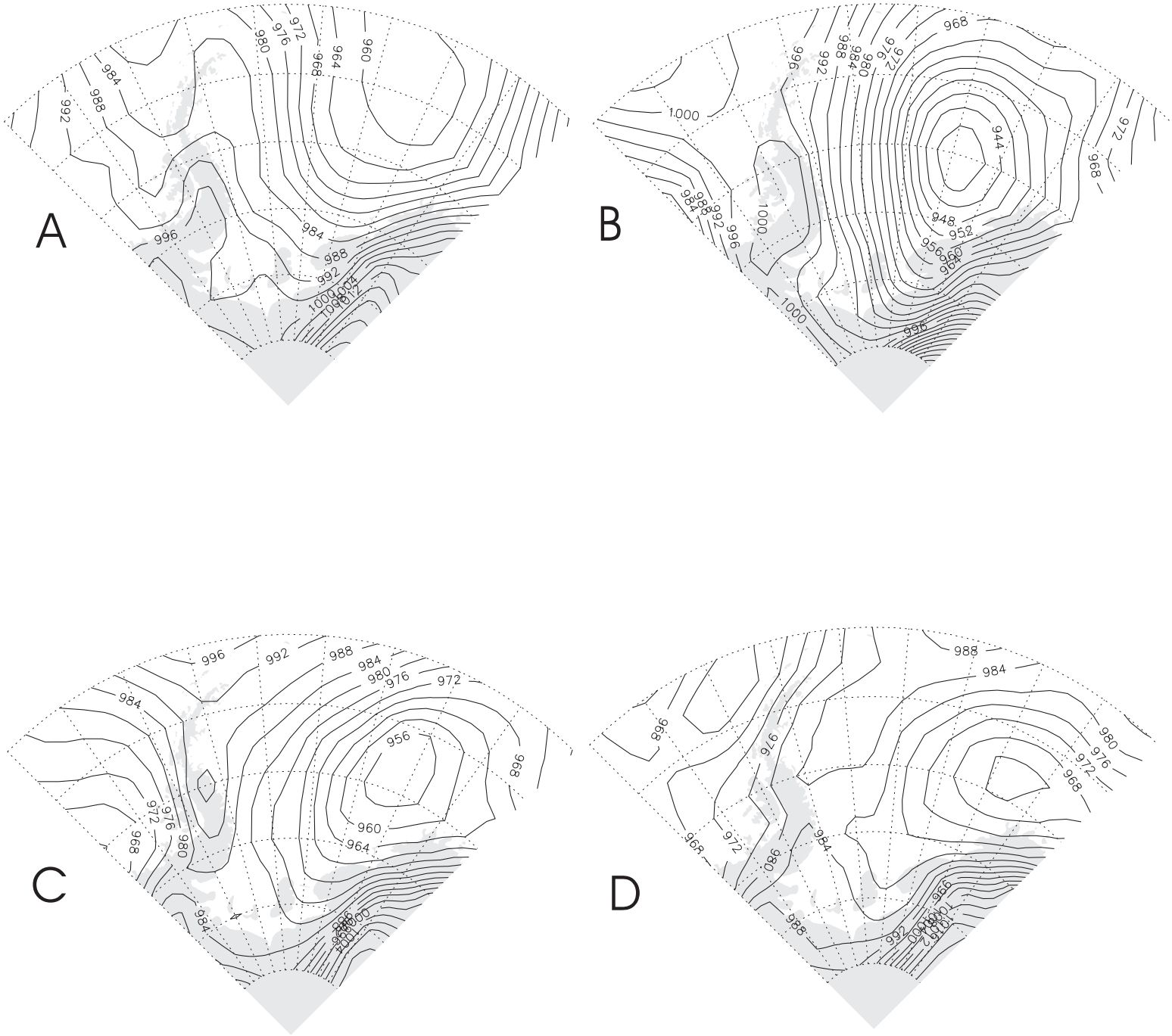


Figure 8 Maps of mean-sea-level pressure for the Weddell Sea region from the NCEP/NCAR reanalyses. The panels show contour plots (interval 4 mb) at 18 UTC on (a) 19th July, (b) 20th July, (c) 21st July and (d) 22nd July 1998.

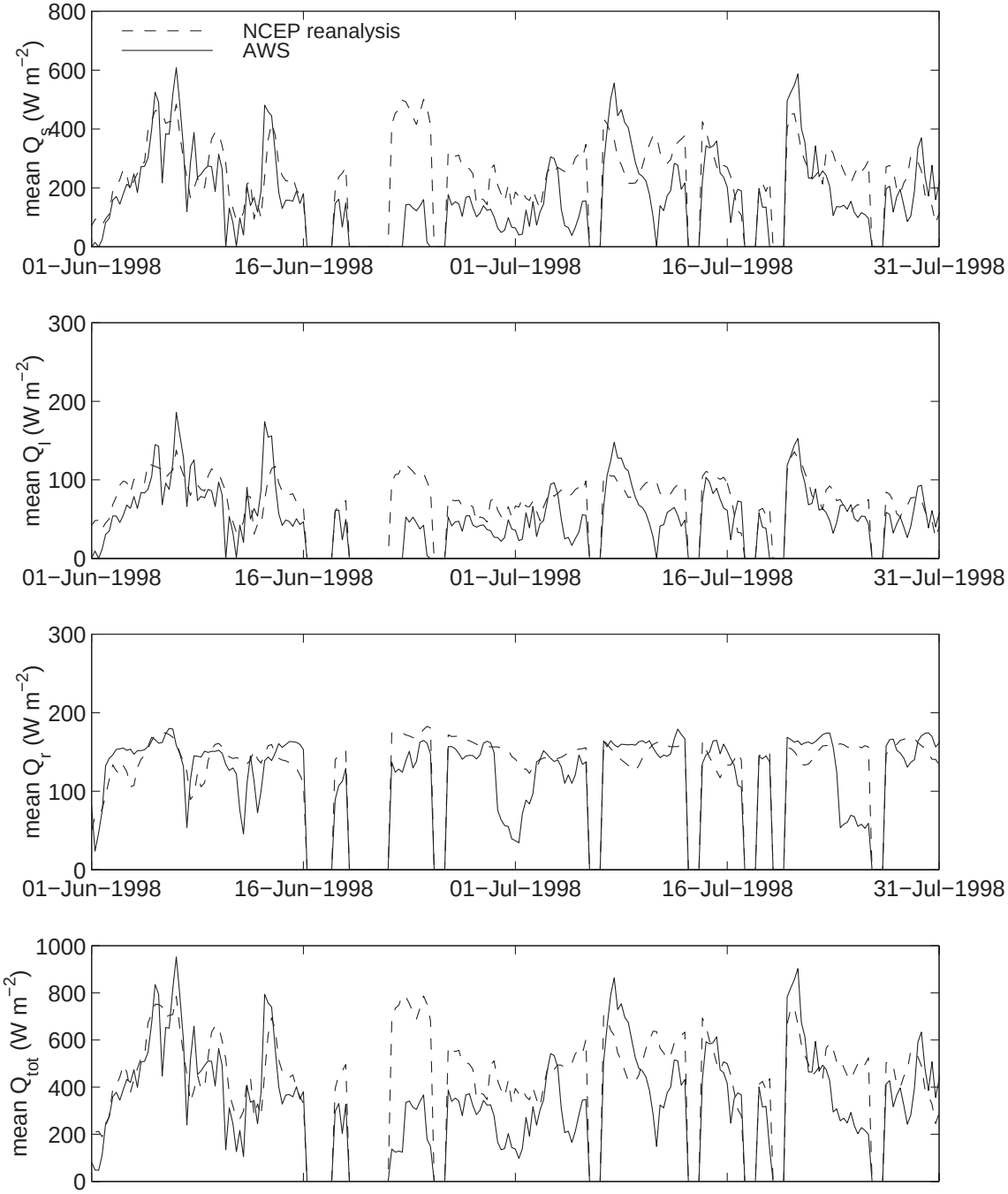


Figure 9 Time series from June-July 1998 showing the coastal-polynya mean surface heat flux components (Q_s, Q_l, Q_r and Q_{tot}) calculated via the NCEP reanalysis and the AWS time series as indicated.

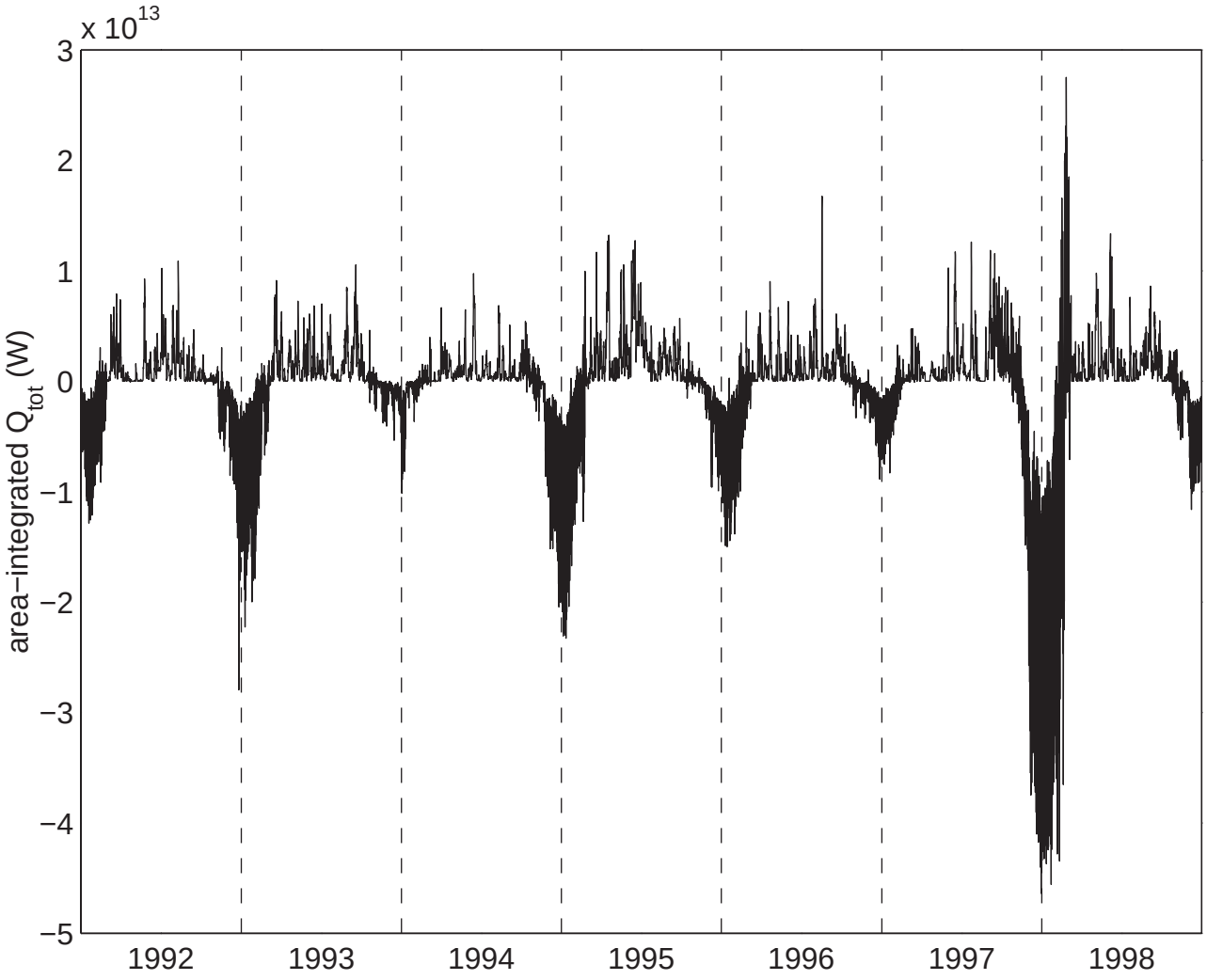


Figure 10 Seven year time series of area-integrated total surface heat flux. Positive values correspond to atmospheric warming (oceanic cooling), negative values correspond to atmospheric cooling (oceanic warming).

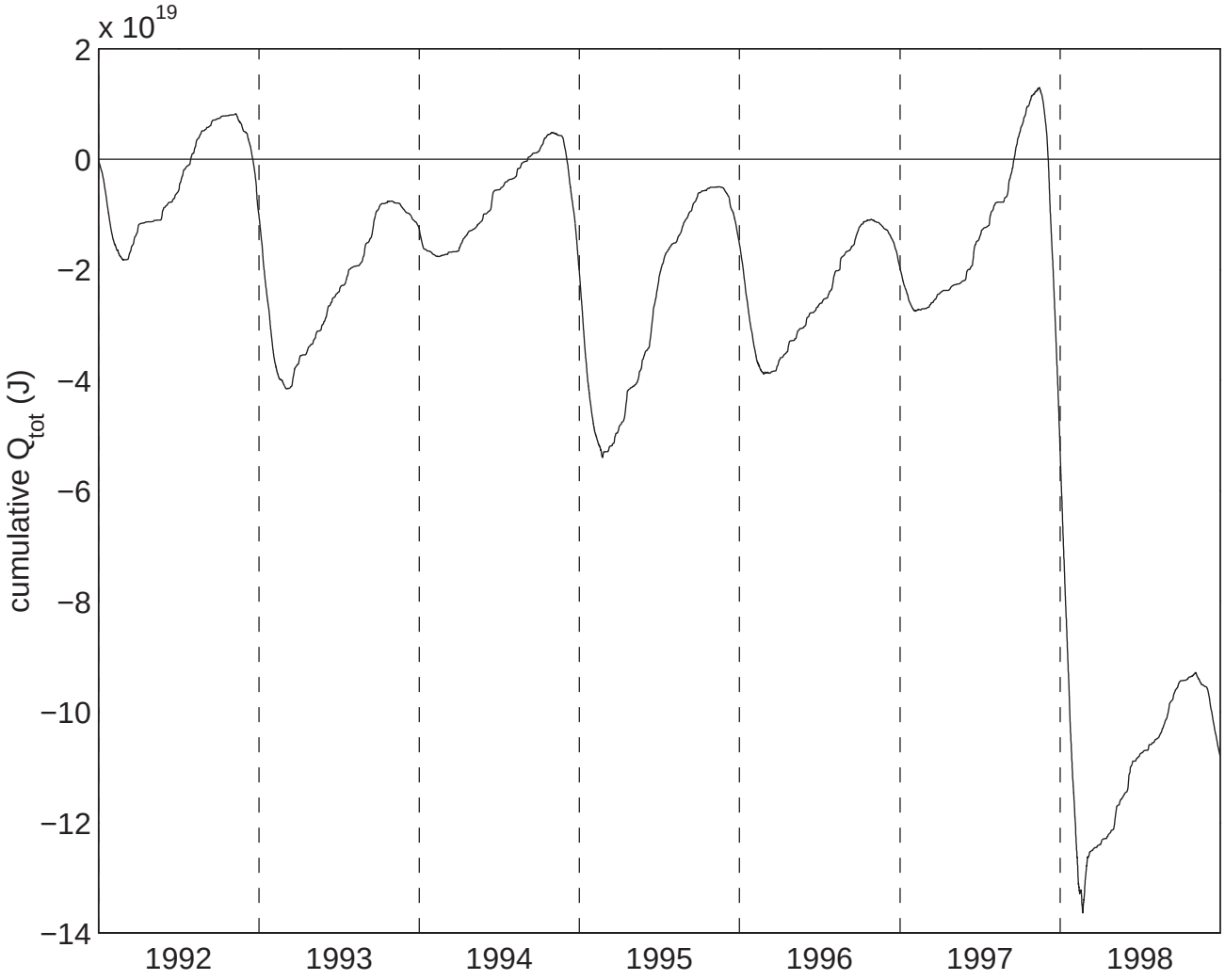


Figure 11 Seven year time series of cumulative area-integrated total surface heat flux, for the coastal polynyas. A positive slope corresponds to the atmosphere gaining energy (the ocean losing energy). The freezing season is defined as the local minimum to the local maximum for each year.

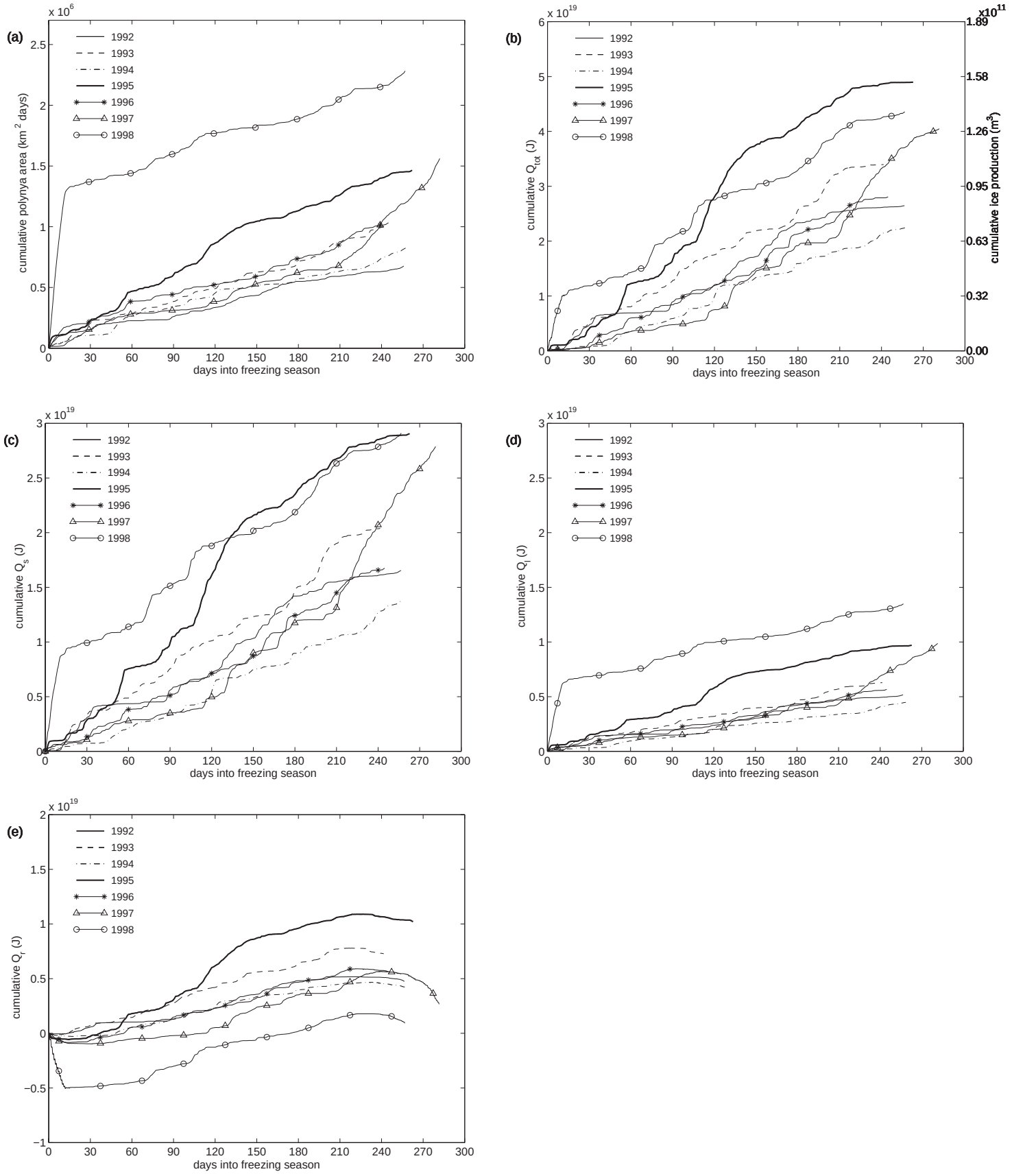


Figure 12 Multi-year time series of each freezing season. The panels show (a) cumulative polynya area, (b) cumulative (area-integrated) Q_{tot}, (c) cumulative Q_s, (d) cumulative Q_l, (e) cumulative Q_r. The start and end dates of the freezing seasons are noted in Table 5.

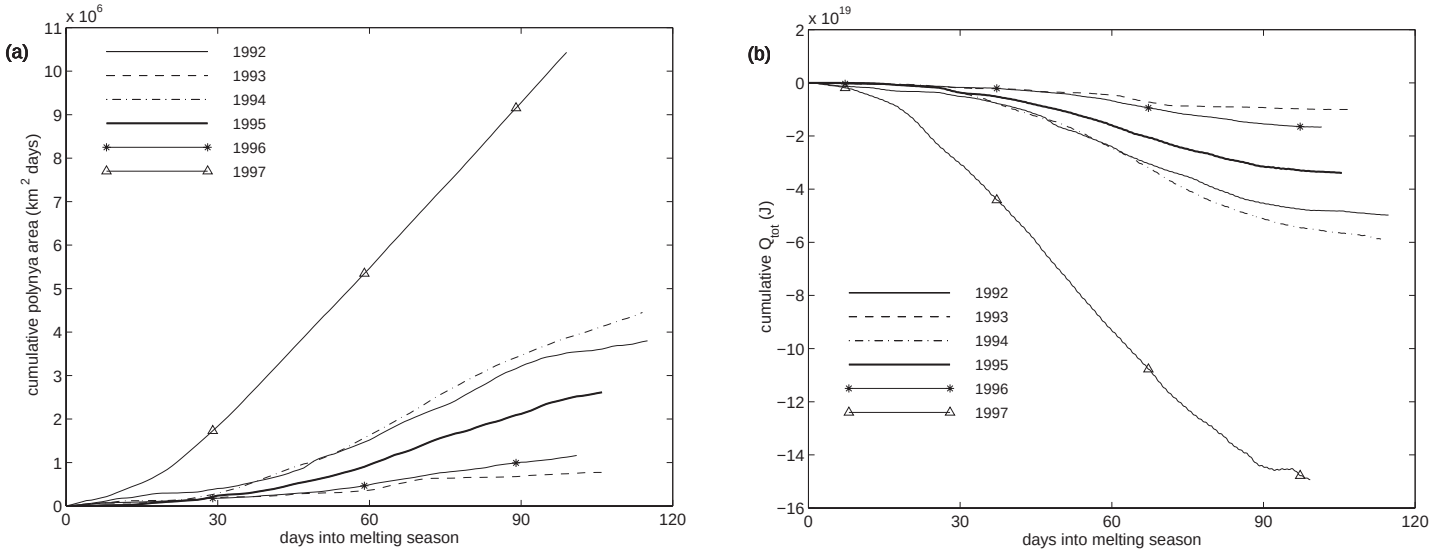


Figure 13 Multi-year time series of each melting season. The panels show (a) cumulative polynya area, and (b) cumulative (area-integrated) Q_{tot}. The start and end dates of the melting seasons are noted in Table 6.

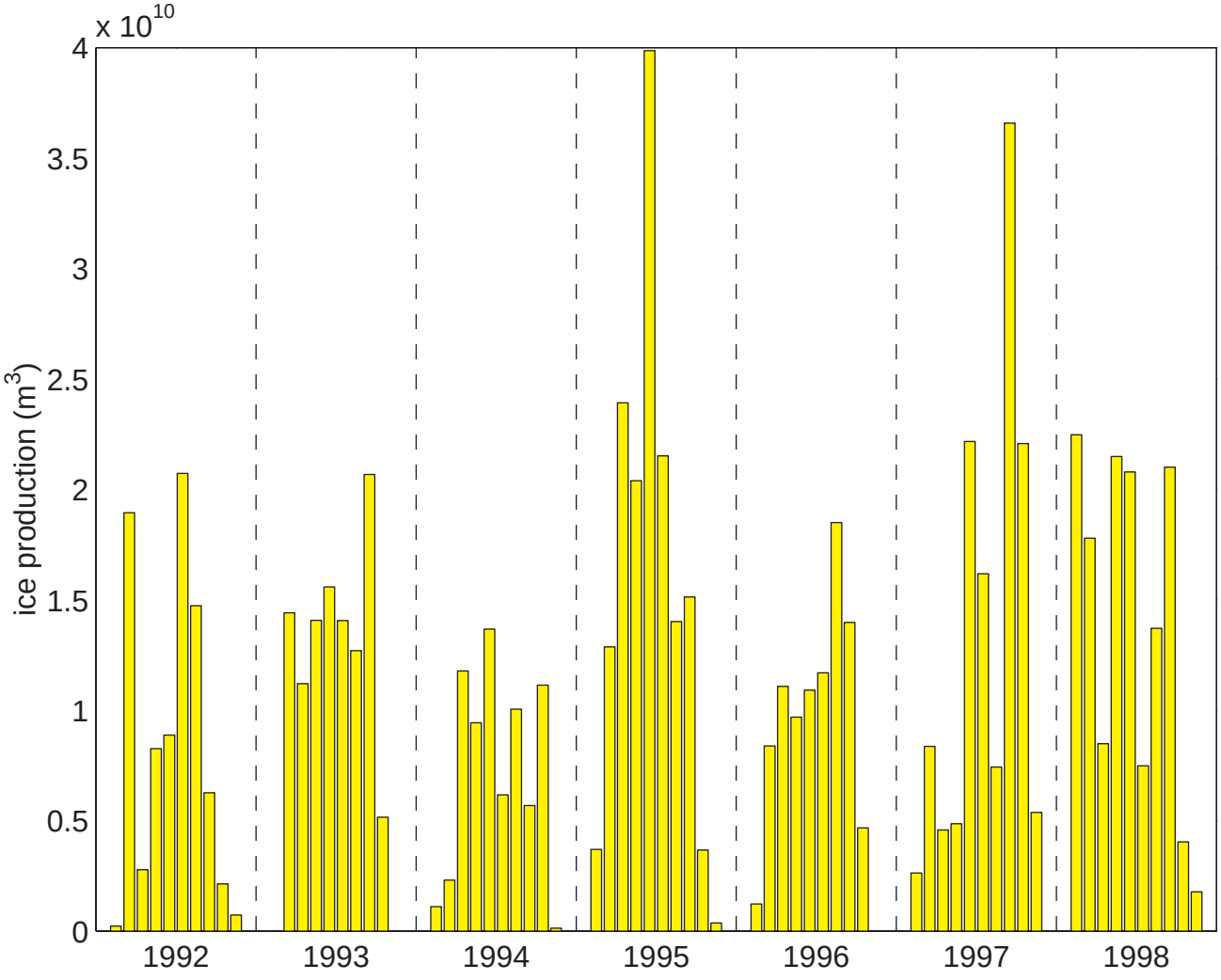


Figure 14 A bar chart of ice production (m^3) for each month of the 7-year climatology. Note there is zero ice production in January, occasionally November, and December of each year.

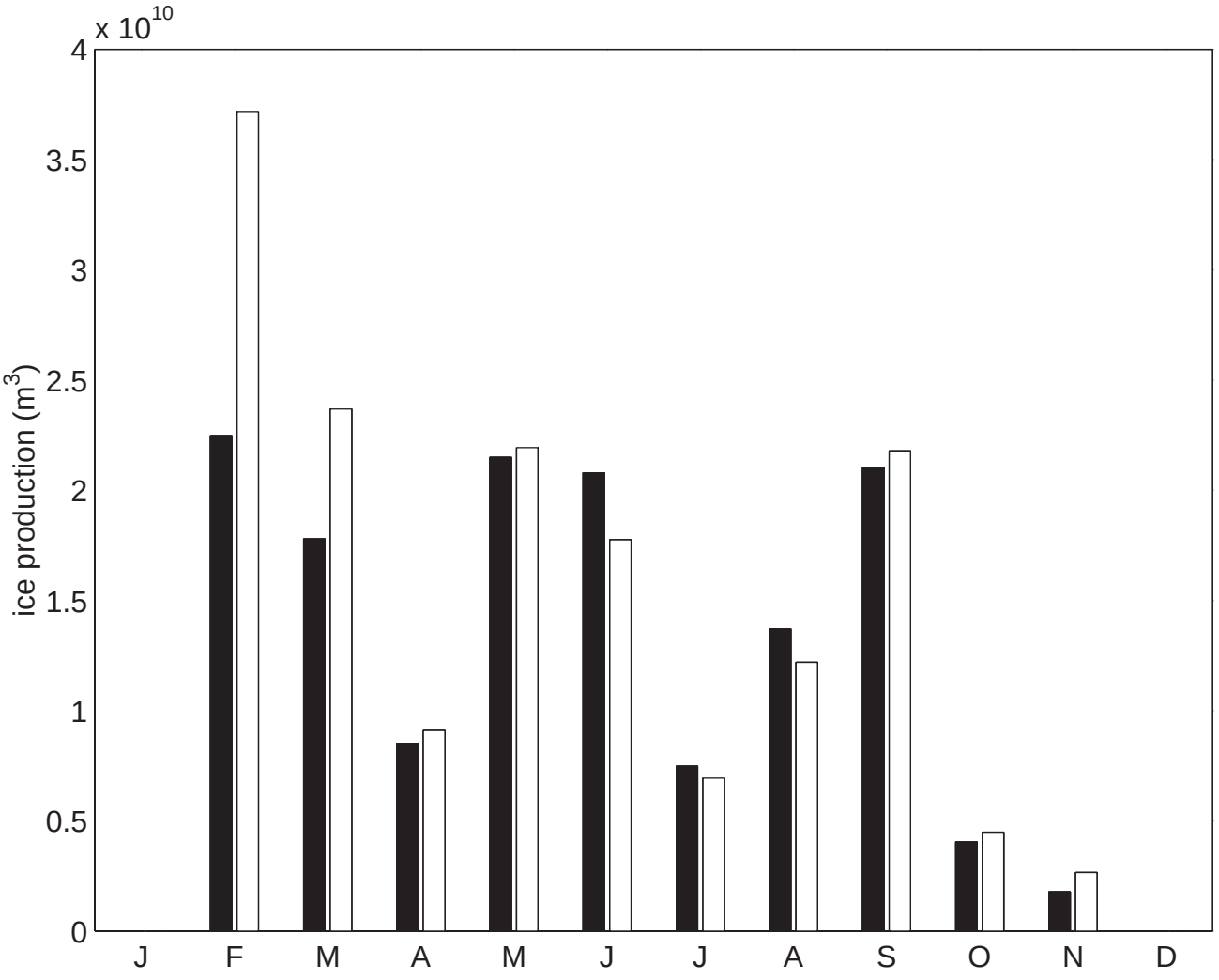


Figure 15 A bar chart of ice production amounts for each month of 1998 using the AWS (open bars) and NCEP (filled bars) meteorological time series as input to the calculation.